地震研究所彙報
Bull. Earthq. Res. Inst.
Univ. Tokyo
Vol. 81 (2006) pp. 317–324

Development of the 7.5-arc-second Engineering Geomorphologic Classification Database and its Application to Seismic Microzoning

Kazue Wakamatsu[1), 2)]* and Masashi Matsuoka[3)]

[1)] Kawasaki Laboratory, Earthquake Disaster Mitigation Research Center, NIED, Kawasaki 210-0006, Japan

[2)] Center for Urban Earthquake Engineering, Tokyo Institute of Technology, Yokohama 226-8502, Japan

[3)] Earthquake Disaster Mitigation Research Center, NIED, Kobe 651-0073, Japan

Abstract

In a seismic hazard assessment, local geologic and ground conditions play important roles in characterizing and estimating hazards. We developed a systematically standardized GIS-based ground-condition map containing the attributes of geomorphologic classification in grid cells of 7.5 arc-seconds latitude×11.25 arc-seconds longitude for several areas including major urban areas in Japan. This paper introduces the concept of developing the 7.5-arc-second JEGM, (Japan Engineering Geomorphologic Classification Map) and presents sample images of the JEGM. As an example of the database's application to estimating the hazards—the average shear velocity of the ground in the upper 30 m,—Vs30 is estimated and mapped for the Kanto area, and the distribution of peak ground velocities (PGV) for the Great 1923 Kanto earthquake is estimated using the Vs30 map and empirical formulae. The computed PGV distribution agrees well with the distribution of seismic intensities evaluated from damage to wooden houses for areas located far from the earthquake fault. However, it will be necessary to calculate ground motion based on an asperity model to evaluate near-fault regions.

Key words : GIS database, geomorphologic classification, seismic hazard mapping, Vs30, PGV

1. Introduction

Several major earthquakes including the Tokai, Tonankai and Nankai earthquakes are expected to occur with high probabilities in the near future in Japan. Local ground conditions play important roles in characterizing and assessing their hazards. However, neither a digital database nor paper maps of ground conditions throughout Japan had been available in a unified form.

Therefore, the authors have created a systematically standardized GIS-based ground-condition map covering all of Japan, the "Japan Engineering Geomorphologic Classification Map (JEGM)" (Wakamatsu *et al.* 2004), which was released in November 2005 (Wakamatsu *et al.*, 2005). The database covers all of Japan with a Japanese standard size grid, which is 30 arc-seconds latitude×45 arc-seconds longitude (approximately 1×1 km^2) and includes five sets of major attributes—geomorphologic classification, geologic age, slope angle, elevation, and relative relief—in approximately 380,000 grid cells. Among its attributes, the geomorphologic classification database was based on a new engineering-based geomorphologic classification scheme for identifying and classifying subsurface ground conditions.

The JEGM was employed for the following types of nationwide hazard mapping: liquefaction potential (Wakamatsu *et al.* 2004), average shear velocity of ground in the upper 30 m, Vs30, for estimating the site amplification factors (Matsuoka *et al.*, 2005), flood potential (Wakamatsu *et al.*, 2005), and erosion rate potential in mountainous area (Hasegawa *et al.*, 2005; Hasegawa *et al.*, 2006a).

To perform more accurate hazard zoning, we

* e-mail: wakamatsu@bosai.go.jp

have been developing a 7.5-arc-second Japan Engineering Geomorphologic Classification Map (7.5-arc-second JEGM) for major areas in Japan, which is a high spatial-resolution version of the above-mentioned 30-arc-second JEGM. In this paper, we present the concept behind the development of the 7.5-arc-second engineering geomorphologic classification database (the 7.5-arc-second JEGM) and its application for seismic hazard estimation.

2. 7.5-arc-second JEGM

(1) Concept of Mapping

The map contains an attribute of geomorphologic classification in grid cells that are 7.5 arc-seconds latitude×11.25 arc-seconds longitude (approximately 250×250 m^2) in size. The criteria for 30 arc-second JEGM were used to develop the 7.5-arc-second JEGM, with some additional classifications such as "lowland between coastal dunes and/or bars," "rock shore, rock reef," and "dry river bed," which are negligible areas in the 1-km square grid cell. A description of geomorphologic map units is presented in Table 1, together with the corresponding general ground conditions and general depth of groundwater. These criteria were based on the purpose of the mapping project: identification and classification of subsurface ground conditions, through standard geomorphologic classification.

The geomorphologic factors presented in Table 1 are known to be correlated with subsurface ground and hydrologic conditions (e.g. Zuidam *et al.*, 1986). Figure 1 shows, for example, typical profiles of boring log, SPT N-values, and elastic wave velocities for three geomorphologic units consisted of sandy soils: marine bar, dune, and natural levee. The profiles are significantly different based on geomorphologic process and/or sedimentary environment of each unit: marine bar generally consisted of moderately dense to dense sands and/or gravelly sands associated with higher N-value and faster elastic wave velocity; dune formed by aeolian processes consisted of loose fine to medium sands associated with low N-value and slow elastic wave velocity, which is usually underlain by dense marine bar deposits; and natural levee formed by fluvial processes was composed of loose sandy soil which was generally underlain by soft fluvial and/or marine cohesive soils.

These are the results of bar deposits compacted under dynamic loading by ocean waves and coastal currents. By contrast, dune and levee deposits accumulate loosely on the wind and river flow, respectively. These geomorphologic factors therefore directly or indirectly influence the subsurface geotechnical ground conditions, although there are some differences based on regionality.

(2) Procedure of Mapping

First, the preliminary map was compiled; the major geomorphologic units were evaluated and classified on the basis of the 30-arc-second JEGM and interpretation of topographic maps. The detailed geomorphologic surveys of local geomorphologic features at scales of 1 : 50,000 were subsequently performed to delineate units on the basis of the criteria listed in Table 1, based on interpretation and compilation of existing information, which is available from published reports, papers, topographical maps, and other available maps and boring exploration data, in addition to our expertise in geomorphology and geotechnical engineering. Finally, a detailed map was drawn up, and digitized and stored in cells using GIS software. Each cell is assigned to the single geomorphologic unit that occupies the greatest area of the cell when multiple units exist within the cell.

Figures 2 shows the areas for which the 7.5-arc-second JEGM is already constructed; areas of Sapporo, Sendai, Kanto including Tokyo, Chukyo including Nagoya, Kinki including Osaka, Kyoto, and Kobe, and Nankaido including Hiroshima, Okayama, and Matsuyama. Sample images of the 7.5-arc-second JEGM for these areas are shown in Figures 4 to 9, respectively. The legend for these maps is shown in Figure 3. The total number of cells of these maps is approximately 2,457,000, which cover nearly 40% of Japan.

3. Utilization of 7.5-arc-second JEGM for Seismic Hazard Estimation

The 7.5-arc-second JEGM has been used for estimating the average shear velocity of the ground in the upper 30 m, Vs30, amplification factors of peak ground velocities and liquefaction potential for the affected area of the 2004 Niigata-ken Chuetsu earthquake (Wakamatsu and Matsuoka, 2006), and overlay analysis of water supply pipes damaged by the earthquake (Hasegawa *et al.*, 2006b).

In this paper, we present a Vs30 mapping of the Kanto area and distribution of peak ground velocity

Table 1. Description of geomorphologic map units in the 7.5-arc-second JEGM.

Geomorphologic map unit	Definition and general characteristics	Subsurface soil condition	General depth of groundwater*
Mountain	Steeply to very steeply sloping topography with highest elevation and relative relief within a grid cell of more than approximately 200 m. Moderately to severely dissected.	Pre-Quaternary hard to soft rock.	Deep
Mountain footslope	Gently sloping topography adjoining mountains and composed of material sourced from the mountains such as colluvium, talus, landslide, and debris flow deposits.	Loose debris and soils consisting of colluvium, talus, landslide, and debris flow deposits.	Deep
Hill	Steeply to moderately sloping topography with higher elevation and relative relief within a grid cell of approximately 200 m or less. Moderately dissected.	Pre- Quaternary and Quaternary hard to soft rock.	Deep
Volcano	Steeply to moderately sloping topography with higher elevation and larger relative relief, composed of Quaternary volcanic rocks and deposits.	Quaternary hard to soft volcanic rock and/or deposits.	Deep
Volcanic footslope	Gently sloping topography located around skirt of volcano including pyroclastic-, mud- and lava-flow fields, and volcanic fan produced by dissection of volcanic body. Slightly dissected.	Quaternary loose to dense volcanic deposits consisting of ash, scoria, pumice, pyroclastic flow, lava, debris avalanche, etc.	Deep
Volcanic hill	Moderately sloping topography composed of pyroclastic flow deposits. Moderately to severely dissected.	Loose to moderately loose pyroclastic flow deposits such as ash, scoria, and pumice.	Deep
Rocky strath terrace	Fluvial or marine terrace with flat surface and step-like form, including limestone terrace of emerged coral reef. Thickness of subsurface soil deposits is less than 5 m.	Hard to soft rock.	Deep
Gravelly terrace	Fluvial or marine terrace with flat surface and step-like form. Covered with subsurface deposits (gravel or sandy soils) more than 5 m thick.	Dense gravelly soil.	Deep
Terrace covered with volcanic ash soil	Fluvial or marine terrace with flat surface and step-like form. Covered with cohesive volcanic ash soil more than 5 m thick.	Stiff volcanic ash (cohesive soil).	Deep
Valley bottom lowland	Long and narrow lowland formed by river or stream between steep to extremely steep slopes of mountain, hill, volcano, and terrace.	Moderately dense to dense gravel or boulder in mountain, but loose sandy soil to very soft cohesive soil in plain.	Shallow
Alluvial fan	Semi-cone-like form composed of coarse materials, which is formed at the boundary between mountains and lowland. Slope gradient is more than 1/1000.	Dense gravel with boulders to moderately dense sandy gravel.	Deep in the central part of fan but shallow in the distal part of fan
Natural levee	Slightly elevated area formed along the riverbank by fluvial deposition during floods.	Loose sandy soil.	Shallow
Back marsh	Swampy lowland formed behind natural levees and lowlands surrounded by mountains, hills, and terraces.	Very soft cohesive soil containing peat or humus.	Very shallow
Abandoned river channels	Swampy shallow depression along former river course with elongate shape.	Very loose sandy soil occasionally covered with soft cohesive soil.	Very shallow
Delta and coastal lowland	Delta: flat lowland formed at the river mouth by fluvial accumulation. Coastal lowland: flat lowland formed along shoreline by emergence of shallow submarine deposits, including discontinuous lowlands along sea- or lake- shore.	Loose fluvial sandy soil over-lying very soft cohesive soil.	Shallow
Marine sand and gravel bars	Slightly elevated topography formed along shoreline, composed of sand and gravel, which was washed ashore by ocean wave and/or current action.	Moderately dense to dense marine sand or gravel occasionally with boulder.	Shallow
Sand dune	Wavy topography usually formed along shoreline or river, comprised of fine to moderately aeolian sand; generally overlies sandy lowland.	Very loose to loose fine to medium sand.	Deep at crest of dune but shallow near base of dune
Lowland between coastal dunes and/or bars	Swampy lowland formed behind dunes or bars	Very soft cohesive soil containing peat or humus.	Very shallow
Reclaimed land	Former bottom flat of sea, lake, lagoon, or river that has been reclaimed as land by drainage.	Loose sand overlying very soft cohesive soil, sometimes covered with loose sandy fill.	Very shallow
Filled land	Former water body such as sea, lake, lagoon, or river reclaimed as land by filling.	Very loose to loose sandy fill, overlying very soft cohesive soil or loose sandy soils.	Very shallow to shallow
Rock shore, Rock reef	Irregular topography of rock or coral around beach zone.	Pre- Quaternary and Quaternary hard to soft rock	Near sea level
Dry riverbed	Nearly flat, irregular topography without water in normal time.	Loose sandy to gravelly alluvial soil, occasionally with boulders.	Very shallow
River bed	Nearly flat, irregular topography with varying water cover and having erosion and accumulation parts.	Loose sandy to gravelly alluvial soil, occasionally with boulders	
Lake	Inland water body.		
Nearshore waters	Nearshore water body.		

* Deep: deeper than 3 m below the ground surface, Shallow: within 3 m of the ground surface, Very shallow: within 1 m of the ground surface

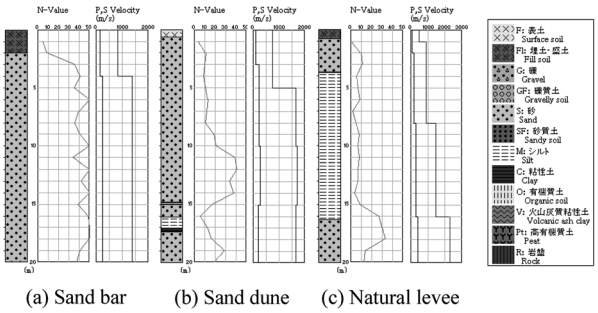

Fig. 1. Typical profiles of boring log, SPT N-values, and elastic wave velocities for three geomorphologic units comprised of sandy soil (Wakamatsu *et al.*, 2004; Borehole data source: National Research Institute for Earth Science and Disaster Prevention, 1997)

(PGV) for the 1923 Kanto earthquake estimated based on the Vs30 map.

In a previous study (Matsuoka *et al.*, 2006), we calculated the Vs30, which is a simple and useful predictor for estimating the site amplification factors of strong ground motions, covering approximately 2,000 sites all over Japan where shear-wave velocity has been measured. Geomorphologic units for all PS logging data sites were interpreted using the original data of the JEGM. Next, we examined the correlation between not only geomorphologic units but also geographical information derived from the JEGM and the Vs30 values. We found that the Vs30s showed some dependency on altitudes, slopes, and distances from mountains or hills formed during older periods (Pre-Tertiary or Tertiary). A multiple linear regression formula for each geomorphologic unit was developed to estimate the Vs30 using elevation (*Ev*), slope (*Sp*), and distance (*Dm*) from a mountain or a hill as explanatory variables. The basic regression formula is the following equation:

$$\log \mathrm{VS30} = a + b \log Ev + c \log Sp + d \log Dm \pm \sigma \quad (1)$$

where *a, b, c,* and *d* represent regression coefficients, and σ is the standard deviation. The units of *Ev, Sp,* and *Dm* are meters, 1000 times tangent values, and kilometers, respectively. When the value of the explanatory variable is less than 1, we fixed the value as "1."

Table 2 shows the regression coefficients and standard deviation of each geomorphologic unit obtained by regression analysis. The regression coefficients show that the higher the elevation, the steeper the slope, and the shorter the distance from the mountain or the hill, Vs30 values become larger. As for the logarithmic standard deviation for the overall estimation, the estimation formula shown in Equation 1 has a higher accuracy than previous empirical estimations (Matsuoka *et al.*, 2006). Using Equation 1 and the attributes of the geomorphologic classification in the 7.5-arc-second JEGM, geologic age, elevation, and slope contained in the 30-arc-second JEGM, we were able to compute the Vs30 distribution with 250 m spatial resolution.

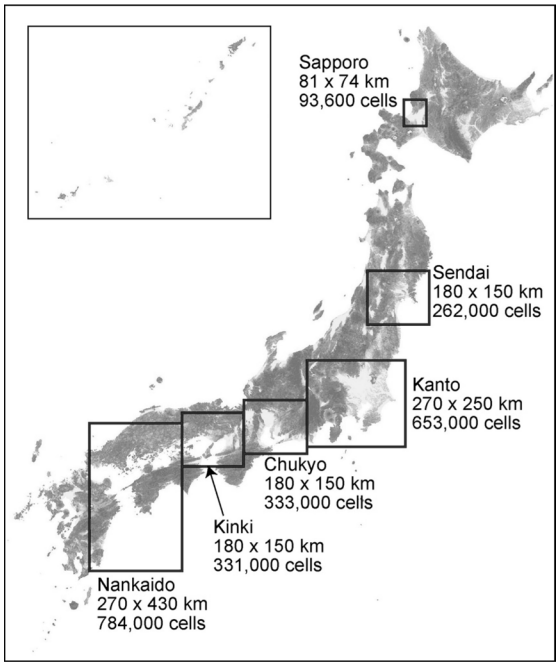

Fig. 2. Areas for which the 7.5-arc-second JEGM is constructed.

Figure 10 shows the Vs30 map for the Kanto area. The Vs30 values are approximately 150 m/s on delta and coastal lowland, reclaimed land, and back marsh. The areas of valley bottom lowland also show a rather small Vs30 in the range from 180 to 200 m/s. To indicate the advantage of the proposed high-resolution Vs30 estimation, the comparison with the previous Vs30 map, which was derived from the 30-arc-second JEGM, is shown in Figure 11. The high-resolution geomorphologic classification of the 7.5-arc-second JEGM enables complicated outlines of geomorphologic map units such as abandoned river channels, natural levee, and valley bottom lowland to be traced. This allows a more realistic Vs30 distribution to be created, as shown in Figure 11 (a).

Fig. 3. Geomorphologic Classification in the 7.5-arc-second JEGM (legend for Figures 4 to 9)

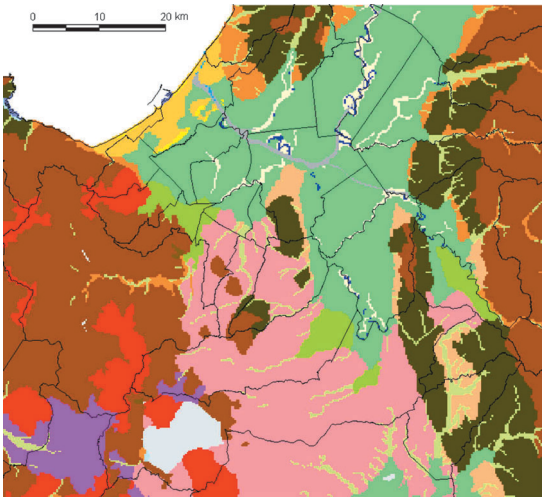

Fig. 4. 7.5 arc-second JEGM for Sapporo area.

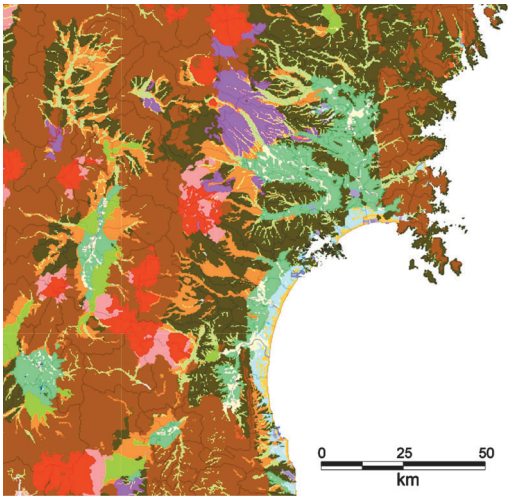

Fig. 5. 7.5 arc-second JEGM for Sendai area.

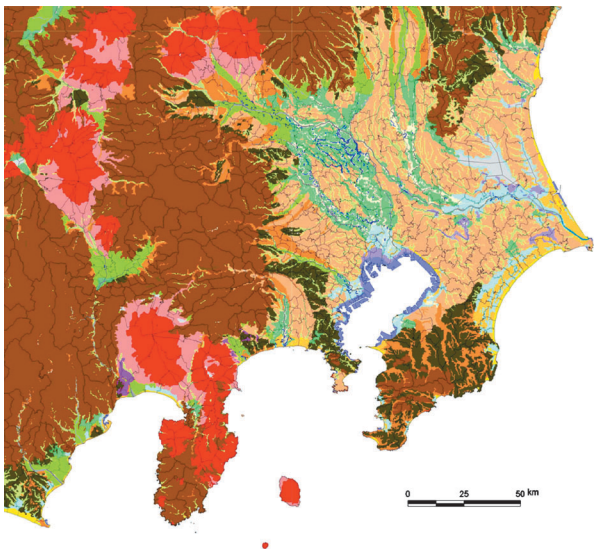

Fig. 6. 7.5 arc-second JEGM image for Kanto area.

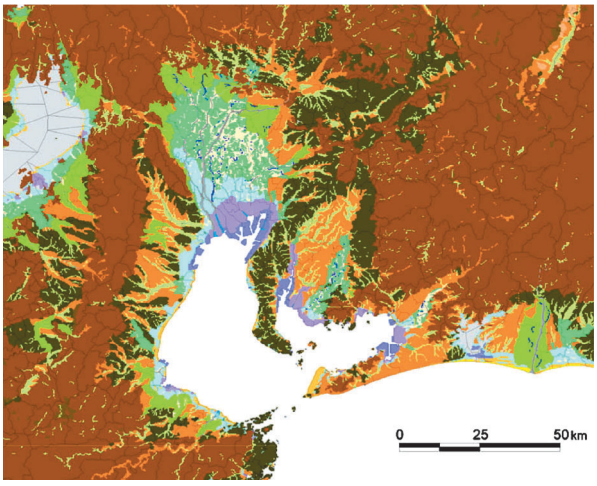

Fig. 7. 7.5 arc-second JEGM for Chukyo area.

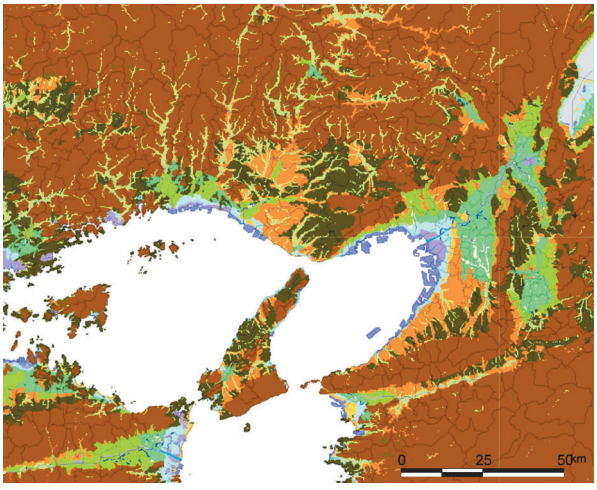

Fig. 8. 7.5 arc-second JEGM for Kinki area.

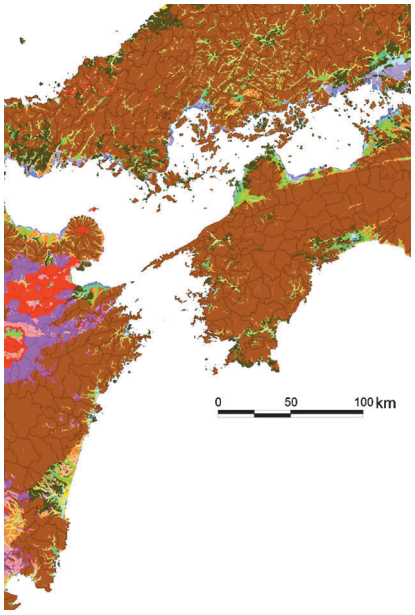

Fig. 9. 7.5 arc-second JEGM for Nankaido area.

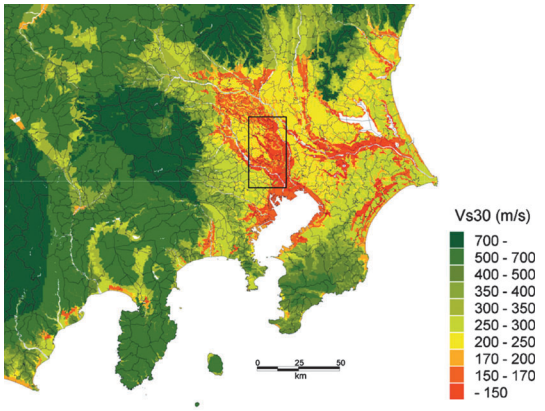

Fig. 10. Vs30 map calculated from the 7.5-arc- second JEGM for the Kanto area.

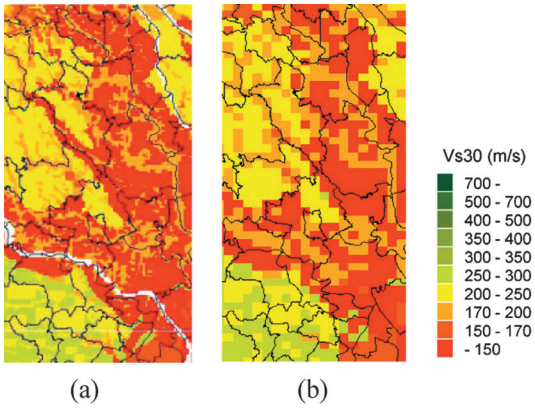

Fig. 11. Zoom-in images (rectangle area in Fig. 10) of Vs30 map for central Kanto area. (a) calculated from the 7.5-arc- second JEGM. (b) calculated from the 30-arc- second JEGM.

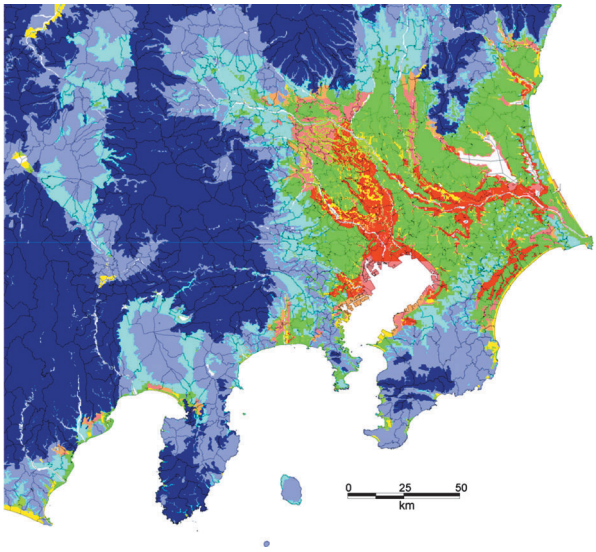

Fig. 12. PGV site amplification map converted from Vs30 map

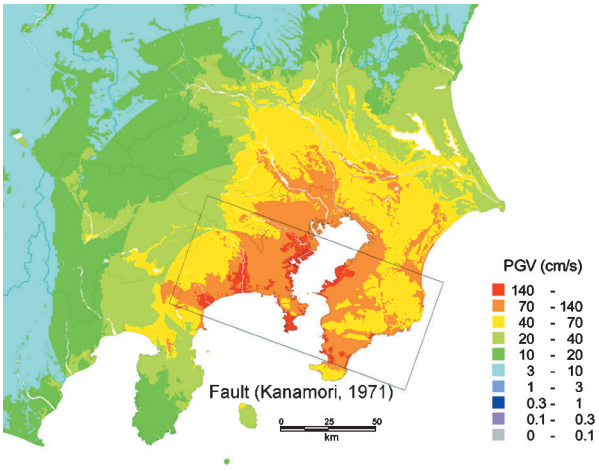

Fig. 13. PGV potential map for the 1923 Great Kanto earthquake using 7.5-arc-second JEGM

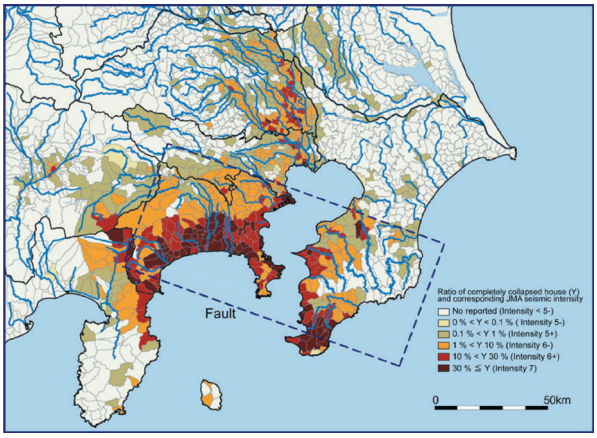

Fig. 14. Distribution of seismic intensity of the 1923 Great Kanto earthquake evaluated from distribution of ratio of collapsed wooden houses (Moroi and Takemura, 2002)

Table 2. Regression coefficient obtained by regression analysis (Matsuoka *et al.*, 2006)

Geomorphologic map unit	Regression coefficient				s.d.
	a	*b*	*c*	*d*	s
Mountain (Pre-Tertiary)	2.900	0	0	0	0.139
Mountain (Tertiary)	2.807	0	0	0	0.117
Mountain footslope	2.602	0	0	0	0.092
Hill	2.349	0	0.152	0	0.175
Volcano	2.708	0	0	0	0.162
Volcanic footslope	2.315	0	0.094	0	0.100
Volcanic hill	2.608	0	0	0	0.059
Rocky strath terrace	2.546	0	0	0	0.094
Gravelly terrace	2.493	0.072	0.027	-0.164	0.122
Terrace covered with volcanic ash soil	2.206	0.093	0.065	0	0.115
Valley bottom lowland	2.266	0.144	0.016	-0.113	0.158
Alluvial fan	2.350	0.085	0.015	0	0.116
Natural levee	2.204	0.100	0	0	0.124
Back marsh	2.190	0.038	0	-0.041	0.116
Abandoned river channel	2.264	0	0	0	0.091
Delta and coastal lowland	2.317	0	0	-0.103	0.107
Marine sand and gravel bars	2.415	0	0	0	0.114
Sand dune	2.289	0	0	0	0.123
Reclaimed land	2.373	0	0	-0.124	0.123
Filled land	2.404	0	0	-0.139	0.120

To draw an amplification capability map, the Vs 30 was converted into the amplification factor for PGV with respect to stiff soil, which corresponds to ground with Vs30 of 600 m/s, through an empirical relationship (Fujimoto and Midorikawa, 2006). The amplification map for the Kanto area is shown in Figure 12.

The potential for ground motion was obtained by multiplying the amplification capability into ground motion intensity on stiff soil. Figure 13 shows the PGV potential map for the 1923 Great Kanto earthquake (Mw 7.9) using 7.5-arc-second JEGM. In this estimation, the location of the earthquake fault refers to the results of Kanamori (1971), and the PGV on stiff soil was simply estimated from an attenuation relationship proposed by Si and Midorikawa (2000). Figure 14 shows the distribution of seismic intensities of the 1923 Great Kanto earthquake evaluated from the distribution of ratios of collapsed wooden houses. For a macroscopic point of view, the areas were located some distance from the earthquake fault, and the computed PGV distribution is in quite good agreement with the distribution of seismic intensities evaluated from damage to wooden houses. To evaluate near-fault regions, it will be necessary to calculate ground motion based on an asperity model.

4. Conclusion

In this study, we introduce the 7.5-arc-second "Japan Engineering Geomorphologic Classification Map (JEGM)," the high spatial-resolution version of 30-arc-second JEGM, which was based on engineering-based geomorphologic classification standards; the concept and procedure of mapping are described, and the image samples of 7.5-arc-second JEGM for major urban areas in Japan are presented.

As an example of the database's application to detailed and accurate hazard zoning, we estimated and mapped the average shear-wave velocity of the ground in the upper 30 m, Vs30 for the Kanto area. Finally, we present detailed maps of amplification capability for peak ground velocity (PGV) in the area and PGV potential estimation for the 1923 Great Kanto earthquake using the Vs30 map and empirical relationships. The computed PGV distribution is in quite good agreement with the distribution of seismic intensities evaluated from damage to wooden houses for areas located some distance from the earthquake fault. However, it will be necessary to calculate ground motion based on an asperity model to evaluate the near-fault regions.

Acknowledgments

The work presented in this paper was supported

by the Special Project for Earthquake Disaster Mitigation in Urban Areas from the Ministry of Education, Culture, Sports, Science and Technology of Japan. The authors gratefully acknowledged this support. They also thank Prof. S. Midorikawa, Tokyo Institute of Technology for providing us facilities for this research.

References

Fujimoto, K. and S. Midorikawa, (2006). Empirical estimates of site amplification factor from strong-motion records at nearby station pairs, Proceedings of 1st European Conference on Earthquake Engineering and Seismology, Paper No. 251, CD-ROM.

Hasegawa, K., Wakamatsu and M. Matsuoka, (2005). Mapping of potential erosion-rate evaluated from reservoir sedimentation in Japan, *Journal of Japan Society for Natural Disaster Science,* **24-3** (in Japanese with English abstract) 287–301.

Hasegawa, K., K. Wakamatsu and M. Matsuoka, (2006a). GIS-based Nationwide Evaluation of Erosion Rate Potential in Japan, Proc. 2nd Japan-Taiwan Joint Workshop on Geotechnical Hazards from Large Earthquakes and Heavy Rainfall, ATC3-ISSMGE, pp.108–113.

Hasegawa, K., H. Sakai, K. Wakamatsu and T. Sato, (2006b). Damage analysis of water supply pipes due to the Mid-Niigata Earthquake, Proc. 8th U.S. National Conference on Earthquake Engineering, CD-ROM Vol. 1, Paper No. 1163, CD-ROM.

Kanamori, H. (1971). Faulting of the Great Kanto earthquake of 1923 as revealed by seismological data, *Bulletin of Earthquake Research Institute,* **49**, 13–18.

Matsuoka, M., K. Wakamatsu, K. Fujimoto and S. Midorikawa, (2006). Average shear-wave velocity mapping using Japan Engineering Geomorphologic Classification Map, *Journal of Structural Engineering and Earthquake Engineering,* **23-1**, 57s–68s.

Moroi, T. and M. Takemura, (2002). Re-evaluation of the damage statistics of wooden houses for the 1923 Kanto earthquake and its seismic intensity distribution, *Journal of Japan Association for Earthquake Engineering,* **2-3**, 35–71(in Japanese with English abstract).

National Research Institute for Earth Science and Disaster Prevention (1997), Soil Data for Kyoshin Net, CD-ROM.

Si, H. and S. Midorikawa, (2000). New attenuation relations for peak ground acceleration and velocity considering effects of fault type and site condition, *Proc. 12th World Conference on Earthquake Engineering,* CD-ROM, ID532.

Wakamatsu, K., M. Matsuoka, K. Hasegawa, S. Kubo, and M. Sugiura, (2004). GIS-based engineering geomorphologic map for nationwide hazard assessment, *Proc. 11th Int. Conf. on Soil Dynamics & Earthquake Engineering and 3 rd Int. Conf. on Earthquake Geotechnical Engineering, San Francisco, CA, USA*. **1**, 879–886.

Wakamatsu, K., S. Kubo, M. Matsuoka, K. Hasegawa, and M. Sugiura, (2005). *Japan Engineering Geomorphologic Classification Map,* University of Tokyo Press (in Japanese with English abstract, GIS data in CD-ROM).

Wakamatsu, K., and Matsuoka M. (2006). GIS-based Japan Engineering Geomorphologic Classification Database for Seismic Hazard Assessment, *Proc. 1st European Conference on Earthquake Engineering and Seismology,* Paper No. 762, CD-ROM.

Zuidam R. A *et al.*(1986). *Aerial Photo-Interpretation in Terrain Analysis and Geomorphologic Mapping,* Smits Publishers, Hague.

(Received December 5, 2005)
(Accepted January 16, 2007)